CHAPTER THREE

Dramatic Acceleration of Electron Flow through Azurin

3.1 ABSTRACT

Re(dmp)$(CO)_3$(H124)/W122/Az(Cu^+) exhibits electron transfer kinetics that are much faster than expected for single-step electron tunneling. We have structurally characterized the system; the orientation of the tryptophan with respect to the phen ligand of the label is suggestive of a pseudo-stacking interaction that may encourage rapid electron transfer from the amino acid to electronically excited rhenium. The change in CO-stretching frequencies throughout the process also allows characterization of ultrafast events using time-resolved infrared spectroscopy. These findings and the characterization of excited rhenium at visible wavelengths with picosecond time resolution have allowed for generation of a model that accounts for the electron transfer events in this system.

3.2 INTRODUCTION

The System

Three β-strands extend from the ligands that coordinate azurin's copper center. The system discussed in this chapter and the next is on the Met121 arm of azurin (**Figure 3.1**). Coordination of the metal is at the 124 site, which is approximately 19 Å away from the copper site. A tryptophan is installed at the 122 site.

Unlike in previously studied tryptophan systems,[1] once oxidized, the tryptophan radical cation was not deprotonated; rather, the subsequent electron transfer from the copper to the radical cation was faster! The two-step electron transfer utilizing this tryptophan radical cation exhibited kinetics much faster than that expected for single-step tunneling. This system is the first metal-modified metalloprotein to empirically demonstrate hopping.

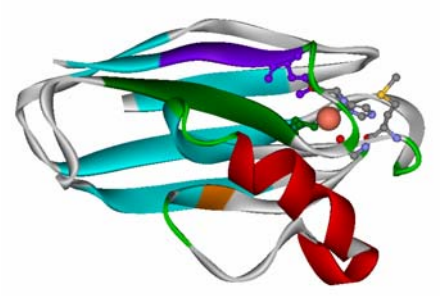

Figure 3.1. *Pseudomonas aeruginosa* azurin (PDB code: 1AZU). The Met121 arm is highlighted in purple.

Chapter Outline

Because this system is the first to exhibit such kinetics, it has been thoroughly characterized in collaboration with a number of laboratories. This chapter will discuss results obtained from these collaborations, as they all contributed in establishing the current model for the electron transfer events of the system. The system has been studied using time-resolved UV-VIS spectroscopy with both 10 ns and 10 ps lasers, time-resolved IR spectroscopy with a 150 fs laser, and structurally characterized by x-ray crystallography. Temperature studies were carried out to assess the thermodynamics of the initial electron transfer between the tryptophan and the rhenium excited state. The results are discussed in the order they were obtained.

Three mutants were prepared for these studies: Re124/W122/Az(Cu^{2+}), Re124/Y122/Az(Cu^{2+}), and Re124/F122/Az(Cu^{2+}). A. Katrine Museth was the first to express and isolate the mutant; Malin Abrahamsson labeled the protein.

A simplified schematic of the events described in the following section is presented below. (**Scheme 3.1**).

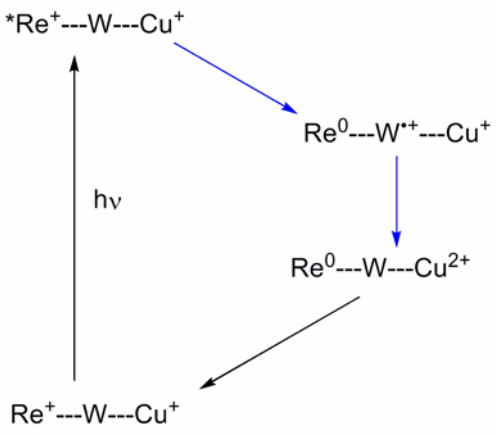

Scheme 3.1. Events after sample excitation. The blue arrows depict the multistep tunneling event.

3.3 RESULTS & DISCUSSION

Proteins for these studies were made using the protocols described in **Chapter 2**. It should be observed here that the rhenium label oxidation states in many of the schemes utilized in this chapter are simplifications: "*Re^{+}" is in actuality *$Re^{2+}(dmp^{\bullet-})(CO)_3$, and that "$Re^{0}$" is in actuality $Re^{+}(dmp^{\bullet-})(CO)_3$.[2]

Time-Resolved UV-VIS Spectroscopy with a 10 ns Laser

Re124/W122/Az(Cu^{+}) was excited with a 10 ns laser. Within 50 ns of sample excitation, formation of Cu^{2+} was observed (**Figure 3.2**, black trace). This is much faster than expected for single-step electron tunneling over a distance ~19 Å! The back ET

reaction can also be tracked; Re^{0} (500 nm, **Figure 3.2**, red trace) and Cu^{2+} kinetics both indicate that it occurs in about 3 μs.

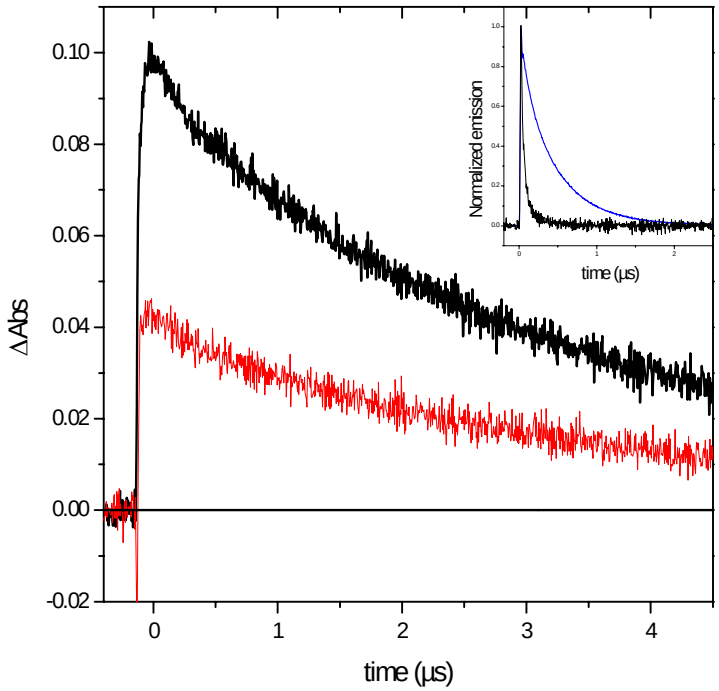

Figure 3.2. Transient absorption of Re124/W122/Az(Cu^{+}). 60 μM Re124/W122/Az(Cu^{+}) in 50 mM KPi pH 7.16. λ_{ex} = 355 nm, λ_{obs} = 628.5 nm (black) and 500 nm (red). Inset: Fluorescence decay at λ_{em} = 595 nm for Re124/W122/Az(Cu^{+}) (black) and Re124/F122/Az(Cu^{+}) (blue)[3]

The quenching of the excited state $*Re^{+}$ is not observed in either Re(H124)/F122/Az(Cu^{+}) or Re(H124)/Y122/Az(Cu^{+}), substantiating the hypothesis that the tryptophan is likely responsible for these enhanced kinetics. Additionally, Cu^{2+} was not formed when Re124/F122/Az(Cu^{+}) or Re124/Y122/Az(Cu^{+}) were excited in similar conditions.

Structural Characterization

A comparison of the x-ray crystal structures of the rhenium-labeled W122 mutant and the rhenium-labeled wild-type K122 variant (**Figure 3.3**) demonstrates a curious and

interesting feature: in the W122 variant (**Figure 3.3B**), the rhenium is oriented such that the dmp ligand is in pseudo π-stacking interaction with the tryptophan residue. The ligand and aromatic ring are within van der Waals contact (~4 Å), which could serve to enhance electron transfer through the tryptophan in an efficient manner. The crystal structure also establishes the distance between the rhenium and copper atoms as 19.4 Å.

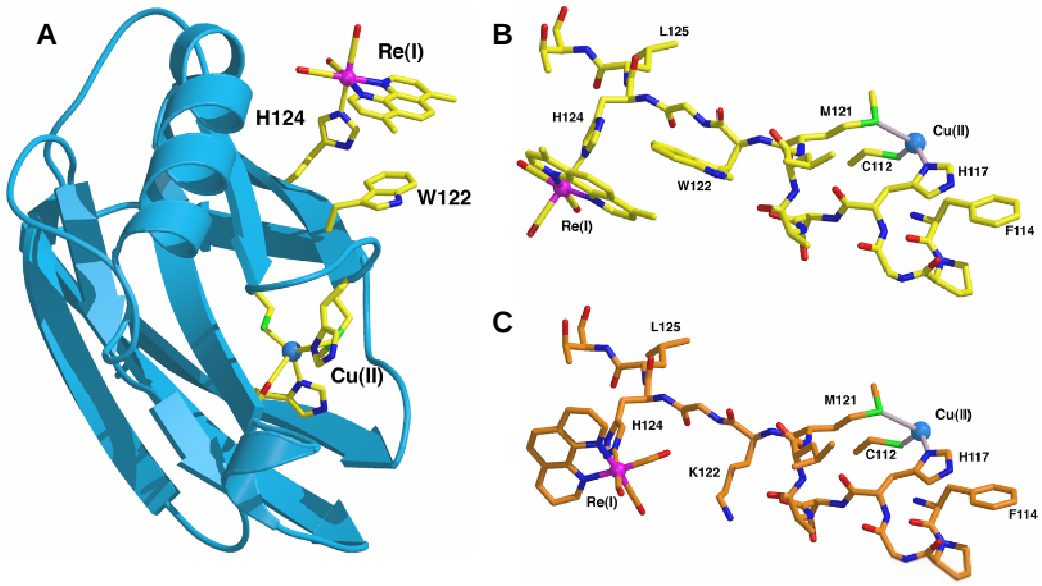

Figure 3.3. Crystal structures of Re-labeled azurins.[3] **A.** Full structure of Re124/W122/Az (Cu^{2+}). **B.** Zoom of area of interest: the electron transfer pathway. **C.** The same area of interest in Re124/Az(Cu^{+}).[3,4]

Time-Resolved IR Spectroscopy

The IR-active CO stretching frequencies of the rhenium ligand offer another mechanism by which to monitor electron transfer events. Samples were excited with a 150 fs laser and monitored using infrared detectors. These ultrafast measurements garnered information on the early events right after photoexcitation (**Figure 3.4**).

The ground state rhenium label's carbonyl stretching frequencies at 1920 and 2030 cm^{-1} are bleached immediately after the excitation. New absorbances instantly

appear and are fully developed at ~1960, 2012, and ~2040 cm^{-1}, which are attributed to the $*^3$Re excited state (denoted MLCT in **Figure 3.4**).[2] The $*^3$Re excited state absorbances decay with several time constants in the range of 10 ps to 50 ns (measured at 1950–1060 cm^{-1}) and the bleach recovers with ~20 ns and ~3 μs kinetics. A small population of Re^0 (denoted ET in **Figure 3.4**) is present within 1 picosecond after excitation. This population continues to grow over time in three phase with time constants of 10 ps, 300–400 ps, and 20–30 ns, followed by a 3 μs decay.

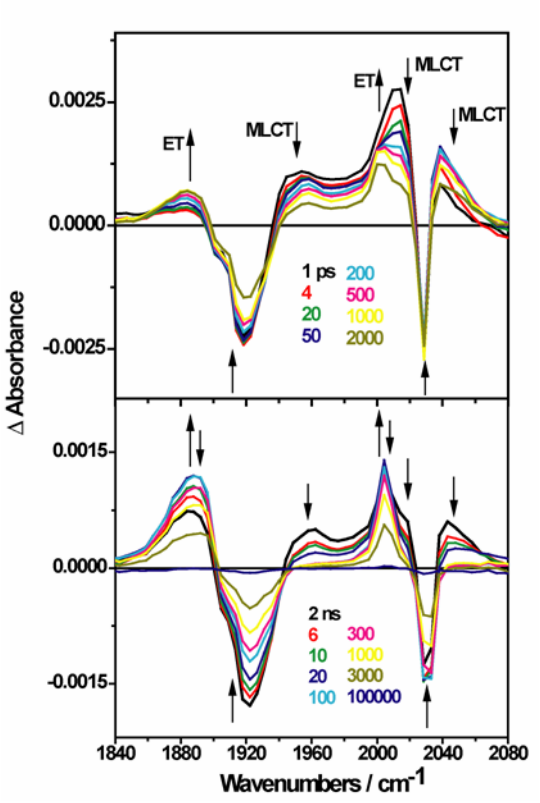

Figure 3.4. Difference time-resolved IR spectra of Re124/W122/Az(Cu^+). Measured in D_2O, pD 7.0 phostphate buffer at selected time delays after 400 nm, ~150 fs excitation. Upper panel: picoseconds. Lower panel: nanoseconds

The measurements made on the other mutants indicated that the tryptophan was absolutely essential for the rapid formation of Re^0: the reduced complex also appeared

when Cu^{2+}- and Zn^{2+}-substituted variants of the mutant were excited, but did not form in studies of Re124/Y122/Az(Zn^{2+}).

Temperature Studies

Because the driving force of the W122 to $*Re^{+}$ electron transfer seemed to be quite low, it was suspected that at lower temperatures, multistep tunneling would be shut down, as the activation barrier would no longer be achieved (**Figure 1.1**). Temperature studies were conducted to confirm this hypothesis.

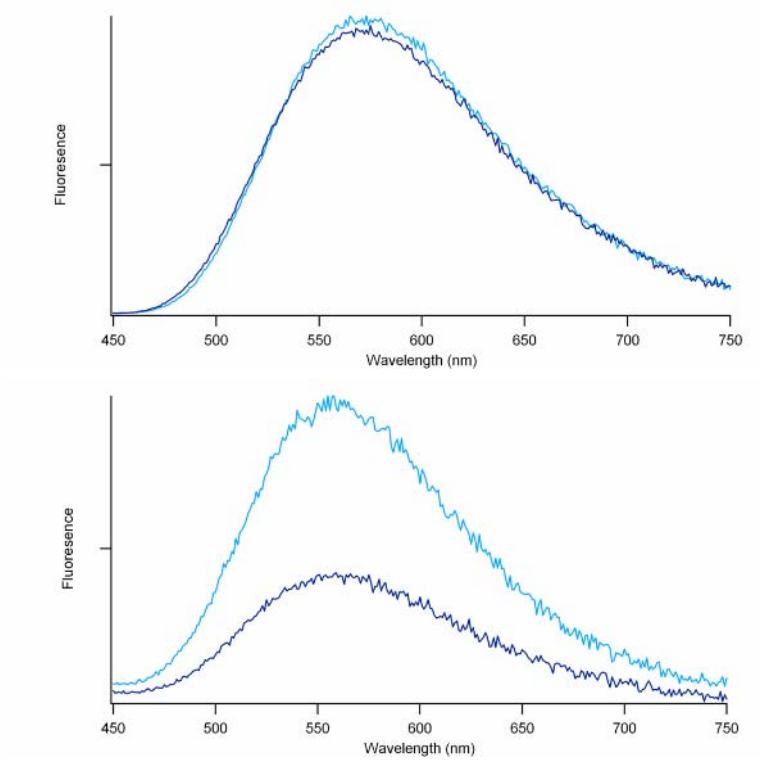

Figure 3.5. Fluorescence spectra of Re (top) and Re124/W122/Az(Cu^{+}) (bottom) at 25°C (dark blue) and -20°C (light blue). ~125 μM Re, 65% glycerol/25 mM KP_i, pH 7.4. 50 μM Re124/W122/Az(Cu^{+}), 65% glycerol/25 mM KP_i, pH 7.4. λ_{ex} = 355 nm

The temperature studies were conducted at room temperature and -20°C, which was the lowest the temperature bath would allow. Glycerol was added to samples as a

cryo-protectant. It can be seen that the temperature change has little effect on the fluorescence of the label (**Figure 3.5, top**). However, for the metal-labeled protein, the fluorescence increases with the decrease in temperature (**Figure 3.5, bottom**). This increase in fluorescence is a sign that the quenching due to the tryptophan is not occurring as much, presumably because the activation barrier is not as easily accessed as it was at room temperature.

Time-Resolved UV-VIS Spectroscopy with a 10 ps Laser

Time-resolved UV-VIS spectroscopy was carried out at faster time scales using a 10 ps laser to furnish more information on the system: fluorescence of the excited state $*Re^{+}$ was monitored with a streak camera.

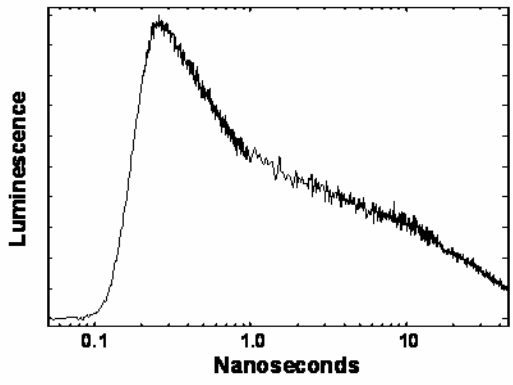

Figure 3.6. Time-resolved emission of Re124/W122/Az(Cu^{+}). 60 μM Re124/W122/Az(Cu^{+}), 50 mM KP_i, pH 7.16. (λ_{ex} = 355 nm, λ_{obs} = 500 nm)

Analysis of this data revealed a biphasic excited-state decay pattern (τ_1 = 400 ps, τ_2 = 26 ns) (**Figure 3.6**). A protocol was developed to deconvolve the instrument response function from the data to garner more accurate fits; the protocol is described below in **Section 3.5**.

The Model

The data obtained from transient absorption, emission, and infrared measurements were fit to **Scheme 3.2** to garner the elementary rate constants for each step of the mechanism. It is gratifying when the data sets for three different spectroscopic methods all fit very well to the same model.

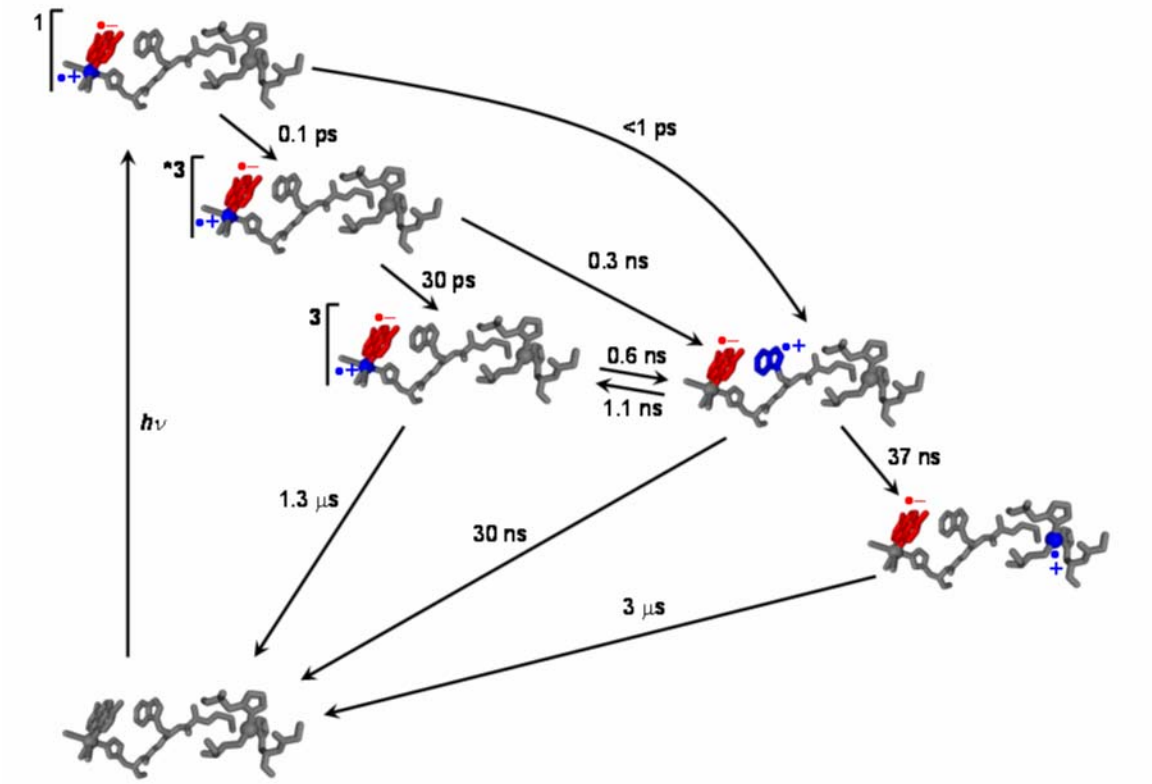

Scheme 3.2. Kinetics model of photoinduced electron transfer in Re124/W122/Az(Cu^+). Light absorption produces electron (red) and hole (blue) separation in the MLCT-excited $*Re^+$. Migration of the hole to copper *via* W122 is complete in less than 50 ns. Charge recombination proceeds on the microsecond timescale.[3] The $*Re^{2+}(dmp^{\bullet-})(CO)_3$ is the more accurate depiction of what has been simplified as "$*Re^+$", and $Re^+(dmp^{\bullet-})(CO)_3$ is the more accurate depiction of the "Re^0" state.

Upon excitation, the $*^{1}Re^{+}$ excited state is generated, which undergoes an extremely fast (~150 fs) intersystem crossing to a triplet excited state $*^{3}Re^{+}$. Subpicosecond generation of Re^{0} is attributable to electron transfer from the W122 to $*^{1}Re^{+}$. The ~10 ps formation of Re^{0} is attributed to a parallel relaxation and reduction of the $*^{3}Re^{+}$ excited state by tryptophan, based on previous work done on other rhenium-modified azurins.[2] No evidence for Re^{0} formation was observed in proteins containing F122 or Y122 mutations; the electron source for these reductions must be the indole of W122. The ~400 ps kinetics phase is attributed to equilibration between $^{3}Re^{+}$ state and Re^{0}-$W^{\bullet+}$ and the ~20 ns process corresponds to reduction of $W^{\bullet+}$ by the Cu^{+} to generate Cu^{2+}.

The analysis of the reaction kinetics reveals that the reduction potential of $*Re^{+}$ is just 14 mV greater than that of $W122^{\bullet+/0}$. This is sufficient for very rapid electron transfer between the adjacent dmp ligand and indole ring. This electron transfer does not occur in the tyrosine and tryptophan mutants because their reduction potentials are more than 200 mV above the the reduction potential of $*Re^{+}$ ($E°(*Re^{+/0})$ = 1.4 V *v.* NHE[5]).

Hopping Map

A true confirmation of the multistep tunneling mechanism was found through the construction of a hopping map (**Figure 3.7**)

Utilizing the distances from the crystallographic data, previously determined λ values, and **Equation 1.1**, a contour map was constructed, depicting the change in overall electron transfer rates if the driving forces of the overall process (x-axis in **Figure 3.7**) and first tunneling step (y-axis in **Figure 3.7**) were varied. The black dot on the graph

represents the potentials of Re(dmp)$(CO)_3$(H124)/W122/Az(Cu^+) system; the calculated value for the process, 87 ns, is within the same order of magnitude of the observed value 37 ns, thereby substantiating our hypothesis that multistep electron tunneling is occurring. Additionally, the two-step hopping is 250 times faster than the calculated single-step tunneling mechanism for the distance and driving force of the Re(dmp)$(CO)_3$(H124)/W122/Az(Cu^+) system.

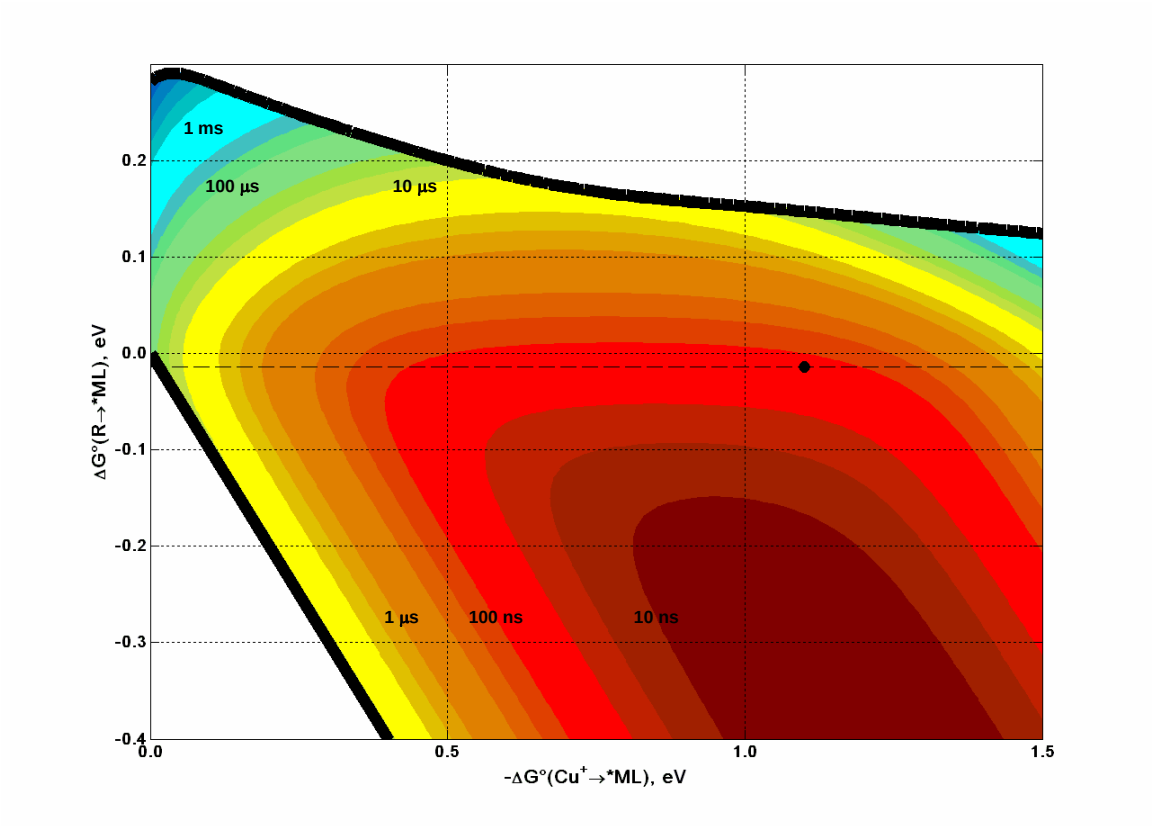

Figure 3.7. Two-step hopping map for electron tunneling through Re-modified azurin. Colored contours reflect electron transfer timescales as functions of the driving forces for the first tunneling step (R→*ML) and the overall electron transfer (Cu^+→*ML). The black dot is located at the coordinates for Re(dmp)$(CO)_3$(H124)/W122/Az(Cu^+). The arrow illustrates the transport time expected if the $Cu^{2+/+}$ potential were high enough to oxidize water.

3.4 CONCLUSIONS

The protein system Re(dmp)$(CO)_3$(H124)/W122/Az(Cu^+) exhibits electron transfer rates that are much faster than expected for a single-step tunneling mechanism. The system was structurally characterized and the kinetics were studied using time-resolved UV-VIS and IR spectroscopies. A multistep tunneling scheme was proposed and the model was fit to the data; the data were all in excellent agreement with the model. Furthermore, a hopping map was constructed to confirm that the theory behind multistep tunneling could accurately predict the electron transfer kinetics of this system. The calculated value was within an order of magnitude of the observed, and the theory is thereby supported by these studies.

3.5 EXPERIMENTALS

Rhenium-labeled proteins were prepared as described in **Chapter 2**.

Collaborators

The substantial amount of data accumulated for this project would not have been accomplished without the help of many collaborators. Crystollographic work was accomplished with Jawahar Sudhamsu and Prof. Brian R. Crane at Cornell University. Time-resolved IR spectroscopy was executed with Ana Maria Blanco-Rodriguez and Prof. Antonín Vlček, Jr. at Queen Mary, University of London, as well as Drs. Kate L. Ronayne and Michael Towrie at the STFC Rutherford Appleton Laboratory. Fits and calculations of the complex systems were done in corroboration with Dr. Jay R. Winkler of the Beckman Institute at Caltech.

Temperature Studies

Temperature studies were carried out on a Fluorolog Model FL3-11 fluorometer equipped with a Hamamatsu R928 PMT and a temperature bath. Samples were prepared and degassed in 1-cm-path-length cuvettes in 65% glycerol/25 mM KP_i, pH 7.4. The sample was excited at 355 nm.

Laser Spectroscopy with a 10 ps Laser

Time-resolved UV-VIS spectroscopy on ultrafast time scales was executed on a customized setup in the Beckman Institute Laser Resource Center. The sample was excited using the third harmonic of a 10 picosecond Nd:YAG laser (Spectra-Physics) at 355 nm (76 MHz, ≤ 5 mW power) and the emission was detected at 90° to the excitation beam using a picosecond streak camera (Hamamatsu C5680). Magic angle conditions were used in the measurements. Rhenium fluorescence was selected with a 420 nm long-pass filter (LPF). The streak camera was used in photon counting mode. Samples were prepared and degassed in 1-cm-path-length cuvettes in the same manner as samples were prepared for laser spectroscopy measurements executed on Nanosecond-I.

Data Analysis

Data obtained from the picosecond laser system was analyzed using MATLAB (The MathWorks). Streak camera images were converted to text files for analysis using the program streak_a.m. A non-negative least-square algorithm was used to fit the data to exponential decays (**Equation 2.1**) (Program max_ent.m). MATLAB programs that were used for data analysis are available in the **Appendix**.

There was concern over whether or not the kinetics observed were too fast for the instrument to detect. Therefore, instrument response was measured and used to deconvolute the data for better fits.

The instrument response was measured by scattering light into milli Q water. Unfortunately some fluorescence was still detected, so the instrument response data was fitted to garner better results for the protocol. The curve was asymmetric, and so was split in half and each half was fit to a Gaussian function (**Figure 3.8**). This function was used as the instrument response curve for the deconvolution protocol.

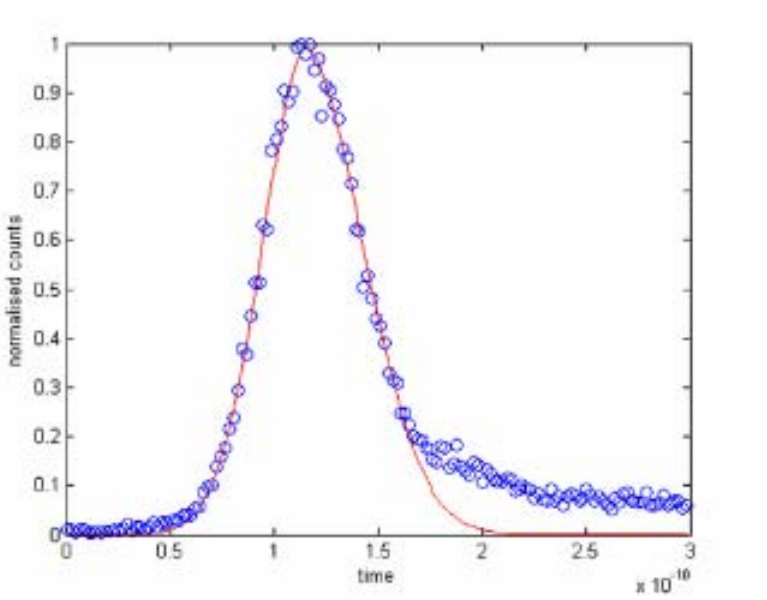

Figure 3.8. Instrument response data fitted to Gaussian functions (red). Data (blue dots) were split in half from the maximum. The early half was fit in its entirety to a Gaussian function. The second half was truncated when it appeared that the fluorescence of the sample was interfering with the response curve.

To convolve the instrument response curve to a theoretical function, MATLAB's 'fminsearch' function was utilized, for which a functions 'crystal' and 'multiexp_conv' were written.

Function 'crystal' took initial guesses of variables, a response vector, an experimental data vector, and a time vector.

Given the initial parameters, function 'crystal' computed a theoretical curve across the given time vector, and then utilized convolved the theoretical curve to a response curve 'O'. O was compared to the experimental data vector and chi square was computed.

MATLAB's 'fminsearch' function changes variables of a function until it minimizes its output value. For this case, the variables changed were summarized in a vector, pram. The 'options' had to be changed to increase the number of iterations to be done; the universal minimum was desired, not a local one.

The function was called with the command:

```
>y=fminsearch(@(x) crystal(x,R,E,t),pram,options)
```

The values for the optimized pram were recalled by running function crystal on pram after the minimization was completed. An example of the output function is shown in **Figure 3.9**.

The fitting procedure discussed here was used as a diagnostic method to check whether or not a more rigorous deconvolution program would need to be written for accurate fitting. The complete protocol undertaken to fit data from all spectroscopic measurements made requires extensive experience and understanding of MATLAB; further fitting was done in heavy collaboration with Dr. Jay R. Winkler.

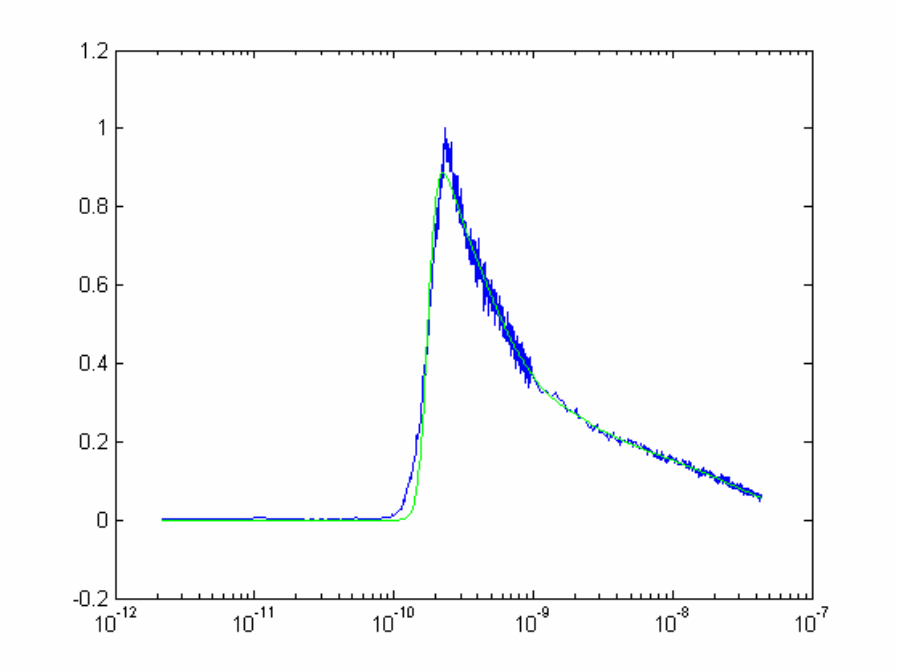

Figure 3.9. A function generated using 'fminsearch' and function 'crystal'. Fit to data collected on Re124/W122/Az(Cu^{+}). Y-axis is normalised emission. Blue is the data to be fitted. Light green curve is the O(t) that was computed to have the lowest chi-square value.

3.6 REFERENCES

(1) Miller, J. E., California Institute of Technology, 2003.

(2) Blanco-Rodriguez, A. M.; Busby, M.; Gradinaru, C.; Crane, B. R.; DiBilio, A. J.; Matousek, P.; Towrie, M.; Leigh, B. S.; Richards, J. H.; Vlcek, A.; Gray, H. B. *J. Am. Chem. Soc.* **2006**, *128*, 4365–4370.

(3) Shih, C.; Museth, A. K.; Abrahamsson, M.; Blanco-Rodriguez, A. M.; Di Bilio, A. J.; Sudhamsu, J.; Crane, B. R.; Ronayne, K. L.; Towrie, M.; Vlcek, A., Jr.; Richards, J. H.; Winkler, J. R.; Gray, H. B. *accepted for publication into Science*.

(4) Sudhamsu, J.; Crane, B. (*personal communication*).

(5) Connick, W. B.; Di Bilio, A. J.; Hill, M. G.; Winkler, J. R.; Gray, H. B. *Inorg. Chim. Acta* **1995**, *240*, 169–173.